Composite Interfaces, Vol. 9, No. 1, pp. 51–60 (2002)

Mechanical damage in carbon fiber polymer-matrix composite, studied by electrical resistance measurement

SHOUKAI WANG and D. D. L. CHUNG *

Composite Materials Research Laboratory, State University of New York at Buffalo, Buffalo, NY 14260-4400, USA

Received 18 December 2000; accepted 9 February 2001

Abstract—The through-thickness resistance of a continuous carbon fiber epoxy-matrix composite laminate was found to be a sensitive indicator of matrix damage. Damage of the matrix between adjacent laminae caused the resistance to change from a behavior in which it reversibly increased with longitudinal strain to one in which it reversibly decreased with longitudinal strain. The longitudinal resistance was a less sensitive indicator of matrix damage. Nevertheless, damage of the matrix between fibers in a lamina caused the longitudinal resistance to decrease gradually and irreversibly.

Keywords: Polymer-matrix; composite; carbon fiber; epoxy; electrical resistance; damage; mechanical.

1. INTRODUCTION

Polymer-matrix composites with continuous carbon fibers are widely used for lightweight structures, such as aircraft, rotating machinery and sporting goods. These composites can be damaged by mechanical forces, whether due to live loads, accidents, wind or other stimuli. Such damage can be a hazard.

Damage monitoring (i.e. structural health monitoring) is valuable for structures for the purpose of hazard mitigation. In practice, damage monitoring does not have to be conducted in real time. However, for studying the process, conditions and reversibility of damage, real-time damage monitoring is desirable.

Damage is conventionally detected by nondestructive methods such as ultrasonic and eddy current methods, which are carried out after the damage infliction rather than during the damage infliction. Observation after the damage infliction allows condition monitoring, whereas observation during the damage infliction enables

*To whom correspondence should be addressed.

better understanding of the cause, mechanism and nature of the damage. Moreover, observation after the damage infliction allows detection of irreversible effects, whereas observation during the damage infliction allows detection of both reversible and irreversible effects. A nondestructive method that is used during damage infliction is acoustic emission [1–4], but this technique does not give information on the reversibility of damage and tends to be sensitive to significant damage only. This paper uses a less common method, namely electrical resistance measurement, for observation during damage infliction [5–24].

Electrical resistance measurement has been previously used to sense strain and damage in carbon fiber polymer-matrix composites. Tensile strain in the fiber (longitudinal) direction of the composite causes the electrical resistivity in the fiber direction to decrease and causes that in the through-thickness direction to increase, due to the increase in fiber alignment in the fiber direction. Damage in the form of fiber breakage causes the electrical resistivity in the fiber direction to increase, whereas damage in the form of delamination causes the resistivity in the through-thickness direction to increase. Hence, electrical resistance measurement allows simultaneous strain and damage sensing. In contrast, acoustic emission detection does not allow strain sensing, unless the strain is associated with damage.

Fiber damage is a more drastic kind of damage than matrix damage, as the fibers are much stronger than the matrix and damage tends to involve the matrix before involving the fibers. Thus, in practical structures, matrix damage is more common than fiber damage. Therefore, this paper is focused on matrix damage.

Previous work on the sensing of matrix damage in carbon fiber polymer-matrix composites by electrical resistance measurement involved measuring the through-thickness resistance [10], as mentioned above. The measurement was conducted during fatigue testing. Matrix damage was observed to start at a third of the fatigue life.

Mechanical damage was observed in previous work during static loading up to failure, during cyclic loading (fatigue), or during repeated loading at increasing stress amplitude [5–24]. However, in this work, damage was observed during repeated loading at increasing and then decreasing stress amplitude within the elastic regime. This form of loading enables distinction between reversible and irreversible effects, both within a stress cycle and within a group of stress cycles with increasing and then decreasing stress amplitude. Thus, new information on the damage evolution and stress history dependence is provided.

Two types of matrix damage were observed in this work. They are (i) matrix damage which allows fibers to touch each other more and results in a decrease in the resistivity, and (ii) matrix damage in the form of matrix cracking or delamination, which results in an increase in the through-thickness resistivity. The first type of damage had not been previously reported in continuous fiber polymer-matrix composites, though it had been reported in short carbon fiber polymer-matrix and cement-matrix composites [25, 26]. The second type of damage is well-known in continuous fiber polymer-matrix composites [10].

Another route for damage monitoring in composites involves embedding sensors, such as optical fibers, in the composite. However, this method is intrusive, in contrast to all of the abovementioned methods, which are non-intrusive.

2. EXPERIMENTAL METHODS

Composite samples were constructed from individual layers cut from a 30.5 cm wide unidirectional carbon fiber prepreg tape manufactured by ICI Fiberite (Tempe, AZ). The product used was Hy-E 1076E, which consisted of a 976 epoxy matrix and 10E carbon fibers. The fiber and matrix properties are shown in Table 1.

The composite laminates were laid up in a 10.2×17.8 cm^2 (4×7 in^2) platten compression mold with laminate configuration [0]. The individual 4×7 in^2 fiber layers (14 per laminate) were cut from the prepreg tape. The layers were stacked in the mold with a mold release film on the top and bottom of the lay-up. No liquid mold release was used. The laminates were cured using a cycle based on the ICI Fiberite C-5 cure cycle. Curing occurred at 355 ± 10°F (179 ± 6°C) and 89 psi (0.61 MPa) for 120 min. The laminates were then cut into pieces of size 175×9.5 mm^2. The density and nominal thickness of the laminate were 1.52 ± 0.01 g cm^{-3} and 1.1 mm respectively after curing. The exact thickness of each specimen cut from the laminate was separately measured in order to determine the longitudinal and transverse resistivities and the longitudinal modulus of the specimen. The volume fraction of carbon fibers in the composite was 58%. Glass fiber reinforced epoxy end tabs were applied to both ends on both sides of each cured piece, such that each tab was 32 mm long and the inner edges of the end tabs on the same side were 110 mm apart and the outer edges were 174 mm apart.

The volume electrical resistance R was measured using the four-probe method while cyclic tension was applied in the longitudinal direction, using a hydraulic

Table 1.
Carbon fiber and epoxy matrix properties (according to ICI Fiberite)

Torayca T-300 (6 K) untwisted, UC-309 sized	
Density	1.76 g cm^{-3}
Tensile modulus	221 GPa
Tensile strength	3.1 GPa
Epoxy	
Process temperature	350°F (177 °C)
Maximum service temperature	350°F (177 °C) dry
	250°F (121 °C) wet
Flexural modulus	3.7 GPa
Flexural strength	138 MPa
T_g	232 °C
Density	1.28 g cm^{-3}

mechanical testing system (MTS 810). Silver paint was used for all electrical contacts. The four probes consisted of two outer current probes and two inner voltage probes. The resistance *R* refers to the sample resistance between the inner probes. Longitudinal and through-thickness *R* values were measured in different samples. For the longitudinal *R* measurement, the four electrical contacts were around the whole perimeter of the sample in four parallel planes that were perpendicular to the stress axis, such that the inner probes were 60 mm apart and the outer probes were 90 mm apart. For the through-thickness *R* measurement, the current contacts were centered on the largest opposite faces and in the form of open rectangles of length 70 mm in the longitudinal direction, while each of the two voltage contacts was in the form of a solid rectangle (of length 20 mm in the longitudinal direction) surrounded by a current contact (open rectangle). Thus, each face had a current contact surrounding a voltage contact. A strain gage was attached to the very center of one of the largest opposite faces, for both longitudinal and through-thickness *R* measurement samples. In the case of the through-thickness *R* measurement sample, the strain gage was at the center of the inner rectangle (voltage contact). A Keithley 2001 multimeter was used. Two specimens were tested for each combination of resistance direction and stress amplitude and reproducibility was found.

3. RESULTS AND DISCUSSION

Figure 1a shows the fractional change in longitudinal resistance during repeated tensile loading at increasing and decreasing stress amplitude. The highest stress

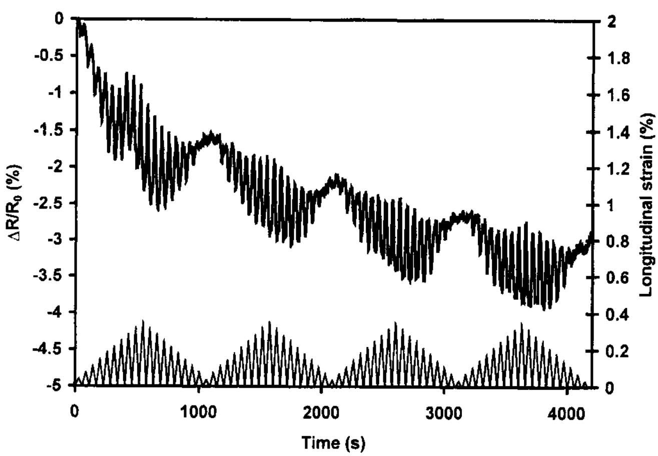

(a)

Figure 1. Fractional change in longitudinal resistance *vs.* time and longitudinal strain *vs.* time during repeated longitudinal loading at a maximum stress amplitude of 53% of the tensile strength. (a) The first four groups. (b) The first group. (c) The second group.

amplitude was 53% of the tensile strength. The strain returned to zero at the end of each cycle for any of the stress amplitudes, indicating elastic behavior. A group of cycles in which the stress amplitude increased cycle by cycle and then decreased cycle by cycle back to the initial low stress amplitude is hereby referred to as a group. Figure 1 shows the results for the first four groups: Fig. 1b shows a magnified view of the first group; Fig. 1c shows a magnified view of the second group. In each cycle of any group, the resistance decreased reversibly upon loading, due to the increase in the degree of fiber alignment, as explained in the Introduction. The higher the stress amplitude, the greater the extent of resistance decrease; this effect was reversible, as shown by comparing the behavior in the first half and second half of a group. However, the baseline resistance decreased as cycling progressed, thus making the reversibility look incomplete. The baseline

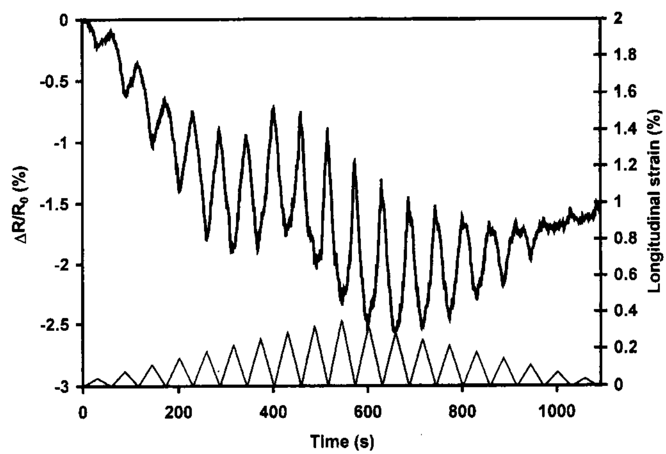

(b)

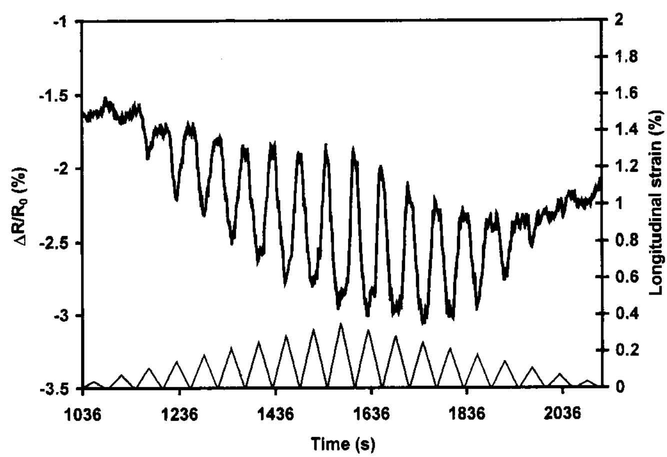

(c)

Figure 1. (Continued).

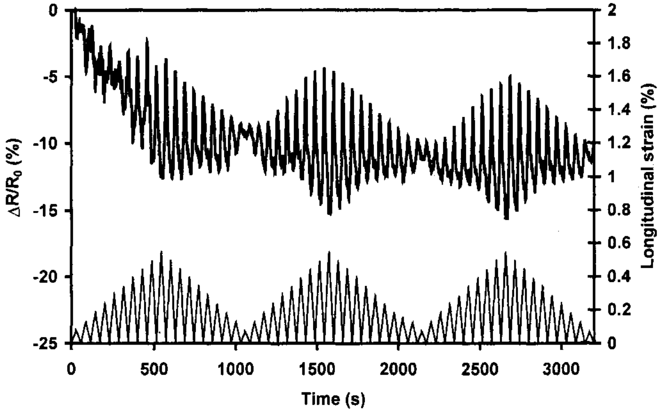

(a)

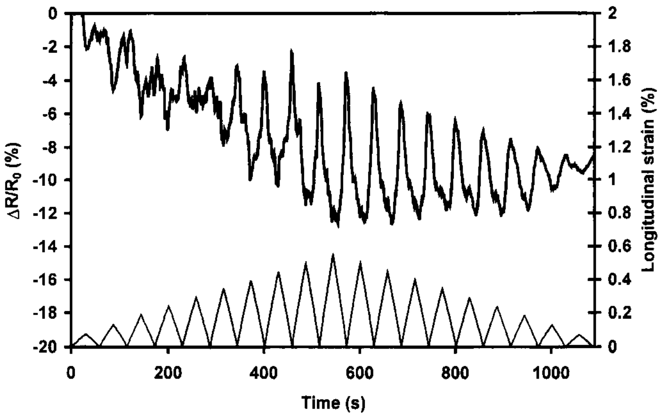

(b)

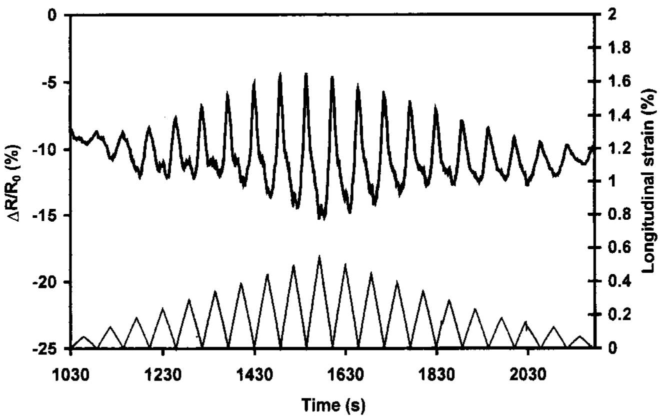

(c)

Figure 2. Fractional change in longitudinal resistance *vs.* time and longitudinal strain *vs.* time during repeated longitudinal loading at a maximum stress amplitude of 71% of the tensile strength. (a) The first three groups. (b) The first group. (c) The second group.

decrease is attributed to minor damage of the matrix. The damage allowed fibers to touch each other more, thus resulting in an irreversible decrease in the longitudinal resistance.

Figure 2a shows longitudinal resistance results for the same situation as in Fig. 1, except that the highest stress amplitude was 71% of the tensile strength. The first three groups are shown in Fig. 2a. The first group is magnified in Fig. 2b; the second group is magnified in Fig. 2c. As in Fig. 1, the resistance decreased reversibly upon loading in every cycle. The higher stress amplitude in Fig. 2 compared to Fig. 1 caused the resistance at the end of a cycle to increase with increasing stress amplitude. This effect was reversible, as shown by comparing the first half and second half of a group. It is attributed to disturbance in the fiber alignment after a cycle and the increasing severity of the disturbance as the stress amplitude increased. This effect was also observed in each of the four groups in Fig. 1, though the effect was weak due to the relatively low stress amplitude. The baseline resistance decreased upon cycling in both Fig. 1 and 2; the fractional decrease was more in Fig. 2 than Fig. 1, due to the higher stress amplitude in Fig. 2.

Figure 3a shows the fractional change in through-thickness resistance during repeated longitudinal tensile loading. The highest stress amplitude was 53% of the tensile strength. The longitudinal strain is shown in Fig. 3, as in all the figures. The stress amplitude is the same in Fig. 1 and 3. The through-thickness resistance (Fig. 3) increased quite reversibly upon loading in each cycle of the first 2.5 groups, due to the increase in the degree of fiber alignment. The higher the stress amplitude, the greater the extent of resistance increase (Fig. 3b and 3c); this effect was reversible. However, in the cycle with the highest stress amplitude in the third group, the resistance decreased reversibly upon loading, in contrast to the resistance increase in earlier cycles (Fig. 3d). In subsequent cycles, the resistance also decreased upon loading, while the noise intensified. In the fourth group, the noise was severe (Fig. 3a). The decrease in through-thickness resistance with increasing strain in a cycle is attributed to major damage of the matrix. This damage, together with the Poisson effect (which squeezed the laminae in the through-thickness direction), caused the fibers in adjacent laminae to touch each other more, thus decreasing the through-thickness resistance. The reversibility is due to the reversibility of the Poisson effect. The increase in noise is also attributed to the damage, which caused the extent of fiber•fiber contacts between adjacent laminae to be less controllable.

The gradual baseline resistance decrease cycle by cycle was observed for the longitudinal resistance (Fig. 1 and 2), but essentially not for the through-thickness resistance (Fig. 3). This means that the minor damage responsible for the gradual baseline decrease is associated with damage of the matrix between the fibers within a lamina. This damage allows greater contact between adjacent fibers in a lamina, thus providing more conduction paths. On the other hand, the major damage responsible for the change from through-thickness resistance increase to through-thickness resistance decrease is associated with damage of the matrix between

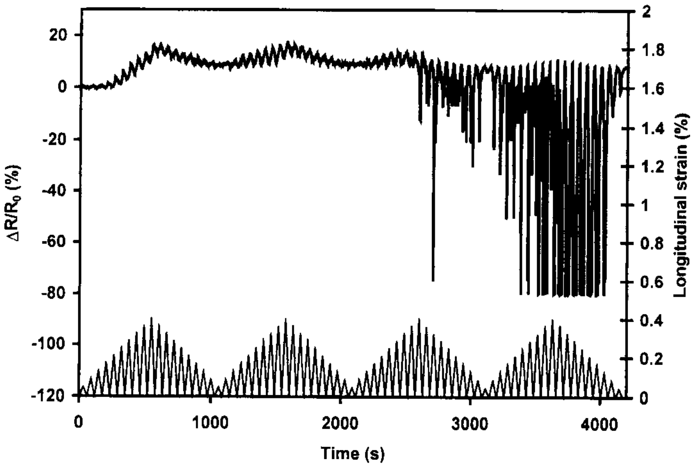

(a)

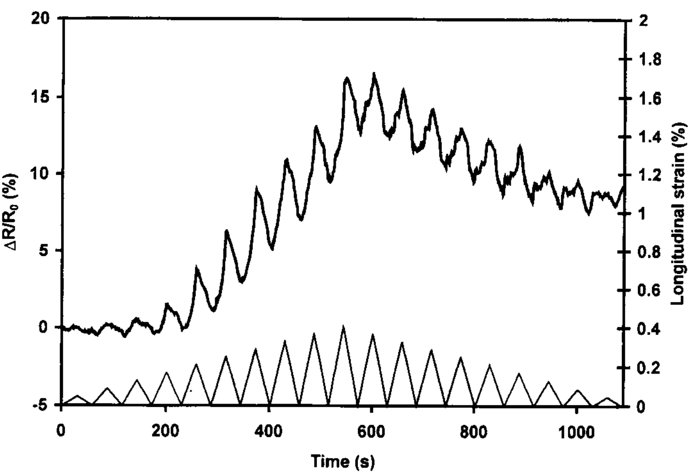

(b)

Figure 3. Fractional change in through-thickness resistance *vs.* time and longitudinal strain *vs.* time during repeated longitudinal loading at a maximum stress amplitude of 53% of the tensile strength. (a) The first four groups. (b) The first group. (c) The second group. (d) The third group.

adjacent laminae. Even more major damage of the matrix between adjacent laminae is responsible for the abrupt increase in the through-thickness resistance baseline, as previously observed during static and fatigue loading [10]. As major damage intensified, the noise associated with the through-thickness resistance measurement became more severe, as previously observed during fatigue loading [10].

The through-thickness resistance is more sensitive to major damage, which occurs between adjacent laminae; the longitudinal resistance is more sensitive to minor damage, which occurs between fibers in a lamina. Both quantities allow damage monitoring in real time, such that the reversible effects due to strain are

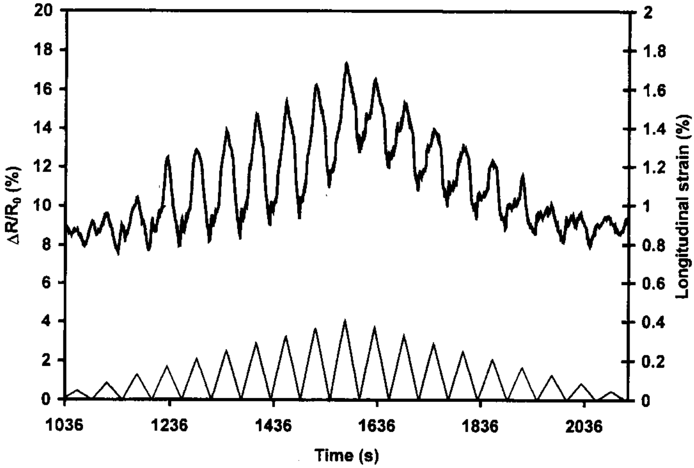

(c)

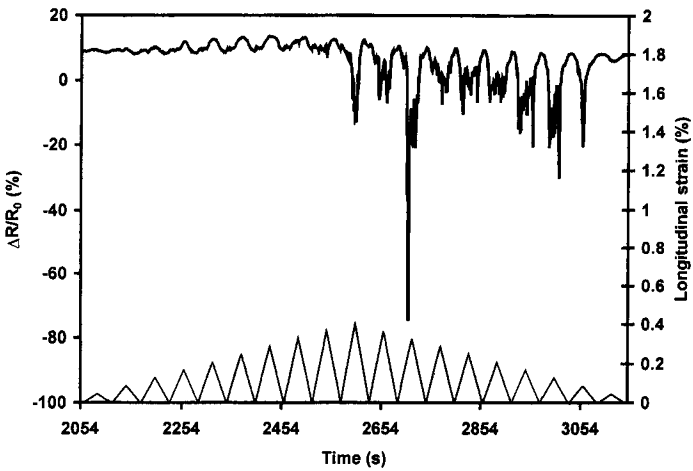

(d)

Figure 3. (Continued).

distinguished from the irreversible effects due to damage. In fact, these quantities also allow strain sensing, as previously reported [7].

4. CONCLUSION

Damage of a continuous unidirectional carbon fiber epoxy-matrix composite laminate upon repeated tensile loading in the fiber direction was monitored in real time by measuring the electrical resistance in either the fiber (longitudinal) direction or the through-thickness direction. Minor damage associated with damage of the matrix between fibers in a lamina caused the longitudinal resistance to decrease gradually and irreversibly upon repeated loading. Major damage associated with damage of the matrix between adjacent laminae caused the through-thickness resistance to change from a behavior in which it reversibly increased with strain to one in which it reversibly decreased with strain.

REFERENCES

1. M. Fuwa, B. Harris and A. R. Bunsell, *J. Phys. D.* **8**, 1460 (1975).
2. M. Fuwa, A. R. Bunsell and B. Harris, *J. Strain Analysis* **11**, 97 (1976).
3. M. Fuwa, A. R. Bunsell and B. Harris, *J. Phys. D.* **9**, 353 (1976).
4. M. Fuwa, A. R. Bunsell and B. Harris, *J. Mater. Sci.* **10**, 2062 (1975).
5. N. Muto, H. Yanagida, T. Nakatsuji, M. Sugita, Y. Ohtsuka and Y. Arai, *Smart Mater. Struct.* **1**, 324 (1992).
6. X. Wang, X. Fu and D. D. L. Chung, *J. Mater. Res.* **14** (3), 790 (1999).
7. X. Wang and D. D. L. Chung, *Composites: Part B* **29B** (1), 63 (1998).
8. P. E. Irving and C. Thiogarajan, *Smart Mater. Struct.* **7**, 456 (1998).
9. X. Wang and D. D. L. Chung, *J. Mater. Res.* **14** (11), 4224 (1999).
10. X. Wang and D. D. L. Chung, *Polymer Composites* **18** (6), 692 (1997).
11. S. Wang and D. D. L. Chung, *Polymer Composites* **21** (1), 13 (2000).
12. X. Wang, S. Wang and D. D. L. Chung, *J. Mater. Sci.* **34** (11), 2703 (1999).
13. N. Muto, H. Yanagida, M. Miyayama, T. Nakatsuji, M. Sugita and Y. Ohtsuka, *J. Ceramic Soc. Japan* **100** (4), 585 (1992).
14. N. Muto, H. Yanagida, T. Nakatsuji, M. Sugita, Y. Ohtsuka, Y. Arai and C. Saito, *Adv. Composite Mater.* **4** (4), 297 (1995).
15. R. Prabhakaran, *Experimental Techniques* **14** (1), 16 (1990).
16. M. Sugita, H. Yanagida and N. Muto, *Smart Mater. Struct.* **4** (1A), A52 (1995).
17. A. S. Kaddour, F. A. R. Al-Salehi, S. T. S. Al-Hassani and M. J. Hinton, *Compos. Sci. Technol.* **51**, 377 (1994).
18. O. Ceysson, M. Salvia and L. Vincent, *Scripta Materiali* **34** (8), 1273 (1996).
19. K. Schulte and Ch. Baron, *Compos. Sci. Technol.* **36**, 63 (1989).
20. K. Schulte, *J. Physique IV*, Colloque C7, **3**, 1629 (1993).
21. J. C. Abry, S. Bochard, A. Chateauminois, M. Salvia and G. Giraud, *Compos. Sci. Technol.* **59** (6), 925 (1999).
22. A. Tedoroki, H. Kobayashi and K. Matuura, *JSME Int. J. Series A — Solid Mechanics Strength of Materials* **38** (4), 524 (1995).
23. S. Hayes, D. Brooks, T. Liu, S. Vickers and G. F. Fernando, in: *Proc. SPIE — the Int. Soc. for Optical Engineering*, Vol. 2718 (*Smart Structures and Materials 1996: Smart Sensing, Processing, and Instrumentation*), pp. 376–384. SPIE, Bellingham, WA (1996).
24. S. Wang and D. D. L. Chung, *Polymer Composites* (in press).
25. X. Shui and D. D. L. Chung, *Smart Mater. Struct.* **5**, 243–246 (1996).
26. X. Fu and D. D. L. Chung, *Cement Concrete Res.* **26** (1), 15–20 (1996).